European Journal of Radiology Open 7 (2020) 100226

Contents lists available at ScienceDirect

European Journal of Radiology Open

journal homepage: www.elsevier.com/locate/ejro

MR imaging of cavernous sinus thrombosis

Harsimran Bhatia*, Ravinder Kaur, Raveena Bedi

Department of Radiodiagnosis Government Medical College and Hospital, Sector 32, Chandigarh, 160030, India

ARTICLE INFO

Keywords:
Cavernous sinus
Thrombosis
Superior ophthalmic vein
Orbit
Orbital apex

ABSTRACT

Purpose: To determine the role of Contrast enhanced MRI (CEMRI) in the evaluation of Cavernous sinus thrombosis (CST).

Method: The study included 7 patients with an imaging diagnosis of cavernous sinus thrombosis. A retrospective analysis of Contrast enhanced MRI of 9 affected cavernous sinuses and a control group of 7 patients (14 cavernous sinuses) was conducted. Various qualitative and quantitative parameters were then compared.

Results: In the patient group, the mean Cavernous sinus (CS) diameter, Cavernous Internal Carotid Artery (ICA) diameter and Superior Ophthalmic Vein (SOV) diameter were 9.14 ± 0.56 mm, 3.5 mm ± 0.9 mm and 3.8 mm ± 1.79 mm respectively. While in the control group, the mean CS diameter, ICA diameter and SOV dimeter were 6.58 ± 0.54 mm, 4.6 mm ± 0.44 mm and 1.1 mm ± 0.11 mm respectively. The differences in the CS size, ICA and SOV diameters was statistically significant. ($p < 0.05$). Cut off points of ≥ 10 mm for CS diameter, ≥ 2.9 mm for SOV dilation, and ≤ 4.2 mm for ICA flow void diameter were estimated using receiver operating characteristic curves. Various other qualitative parameters, like bulging lateral walls of the sinus, heterogenous signal intensity with filling defects on post contrast images, abnormal dural enhancement along the lateral wall of the sinus and orbital apex involvement were more frequently observed in the CST group, in comparison to the control group.

Conclusions: CEMRI plays an invaluable role not only in the diagnosis of cavernous sinus thrombosis, but also in evaluating the extent of disease and its associated complications. The quantitative and qualitative parameters described here, provide more objectivity and accuracy in diagnosis of CST, thus, aiding prompt diagnosis and early treatment.

1. Introduction

Cavernous sinus thrombosis (CST) is a rare and a fulminant life-threatening disorder that can complicate many pathologies affecting the brain and the orbit, having an incidence of about approximately 0.2–1.6 per 100,000 per year [1].

Etiological factors include facial infection, sinusitis, orbital cellulitis, pharyngitis, or otitis, following traumatic injury or surgery. Patients with diabetes, thrombophilia or an immunocompromised state are especially more prone to develop CST [2–6].

Clinical features most commonly include fever and headache along with eye findings such as periorbital swelling, and ophthalmoplegia. Early and prompt recognition of cavernous sinus thrombosis is critical for appropriate and timely management, ensuring good prognosis.

Mortality and morbidity were high in the pre-antibiotic era, but, with the availability and the use of newer antibiotics, the incidence of CST has decreased drastically.

Although the diagnosis is usually clinical, imaging with CT and/or MRI is essential to demonstrate thrombosis, to assess the disease extent and to rule out associated complications.

Imaging helps in identifying thrombosis either via direct visualisation of the thrombus/filling defect in cavernous sinus or via indirect signs that include proptosis, dilatation of the draining tributaries and abnormal dural enhancement, that are well demonstrated on contrast enhanced studies [7–10].

Non-contrast CT of the head, as an initial radiological investigation, may show several subtle abnormalities such as engorgement or dilation of the superior and/or inferior ophthalmic veins, bulging of the lateral margins of the cavernous sinus and possibly the presence of sinusitis, or mass lesions near the sphenoid or pituitary gland, which may indicate an underlying cavernous sinus pathology [11].

Contrast enhanced CT/MRI, in addition to the above mentioned findings shows presence of heterogeneous and asymmetric filling defects, thrombosis in the superior ophthalmic vein, other venous

Abbreviations: CEMRI, Contrast enhanced MRI; CST, Cavernous Sinus Thrombosis; ICA, Internal Carotid Artery; SOV, Superior Ophthalmic Vein; IJV, Internal Jugular Vein; FFE, Fast Field Echo; T1W, T1 weighted image; T2W, T2 weighted image

* Corresponding author.
E-mail addresses: harsimranbhatia13@gmail.com (H. Bhatia), drravinder19@gmail.com (R. Kaur), raveena_bedi@hotmail.com (R. Bedi).

https://doi.org/10.1016/j.ejro.2020.100226
Received 28 October 2019; Received in revised form 11 February 2020; Accepted 22 February 2020

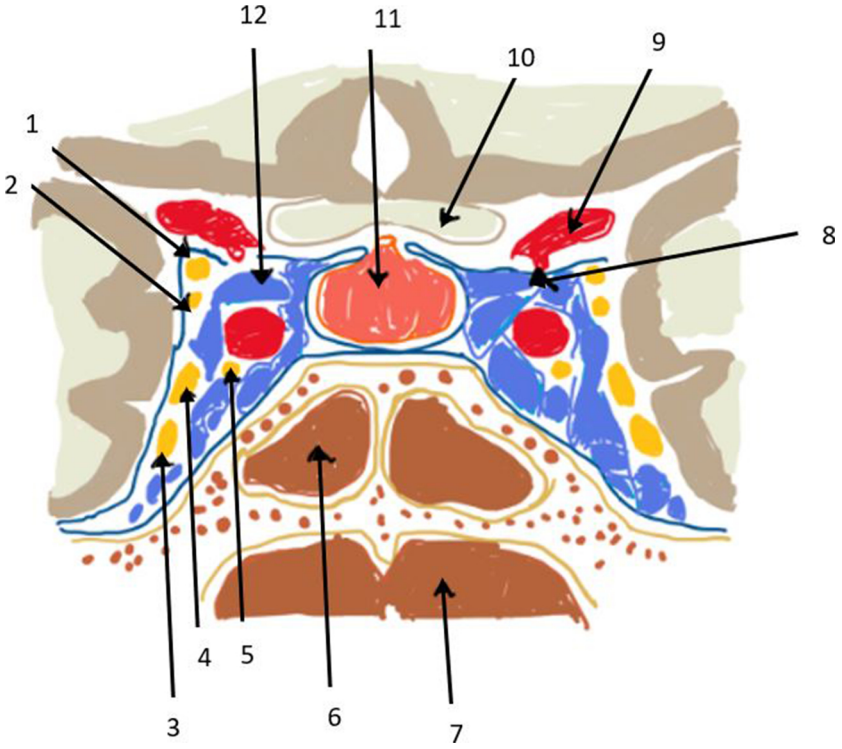

Fig. 1. Diagrammatic illustration of the coronal section of the cavernous sinus anatomy showing(1-10 in anticlockwise direction): 1: Oculomotor nerve (III); 2: Trochlear nerve (IV); 3: Maxillary nerve (V2); 4: Ophthalmic (V1); 5: Abducens nerve (VI); 6: Sphenoid sinus; 7: Nasopharynx; 8: Posterior Communicating artery; 9: Internal carotid artery; 10: Optic chiasm; 11: Hypophysis (Pitutary gland) and 12: Cavernous sinus.

Table 1
Clinical details of the CST group.

S No	Age	Sex	Fever	Headache	Diplopia	Exophthalmos	Decreased vision	Ophthalmoplegia
1	73	M	+	+	–	–	–	+
2	18	M	+	+	+	–	–	+
3	37	F	+	+	+	–	–	–
4	38	M	+	+	+	–	+	–
5	28	F	+	+	+	–	–	–
6	10	F	+	+	+	–	+	+
7	36	F	+	+	+	+	–	+

Table 1 denotes the clinical details of the patients in the CST group.

Table 2
Parameters assessed on imaging.

	Parameters assessed bilaterally:
	Quantitative variables
1	Size of the cavernous sinus
2	Status of the cavernous ICA (diameter and flow void on plain MRI and enhancement on contrast MRI)
3	Status of the Superior Ophthalmic Vein (diameter and flow void on plain MRI and enhancement on post contrast MRI)
	Qualitative variables
1	Lateral wall (margin) of the sinus
2	Signal intensity on plain MRI
3	Filling defect(s) on post contrast MRI
4	Dural enhancement along lateral wall of the sinus
5	Presence of proptosis
6	Involvement of the orbital apex
7	Preseptal involvement

Table 2 denotes the parameters (both qualitative and quantitative) that were assessed on MRI.

tributaries, dural venous sinuses and cerebral veins, which is essential to know, as multiple thrombosis are commonly associated with this condition. This is important in deciding upon the need of anticoagulation and surgical management, required, if any. Additionally, orbital involvement as denoted by abnormal orbital fat density/signal intensity, is well denoted along with other features like narrowing of the carotid artery, carotid arterial wall enhancement, and other intraparenchymal abnormalities like cerebral infarcts, empyema, meningitis, cerebritis and abscess [12–16].

The aim of this retrospective study was to study the accuracy of

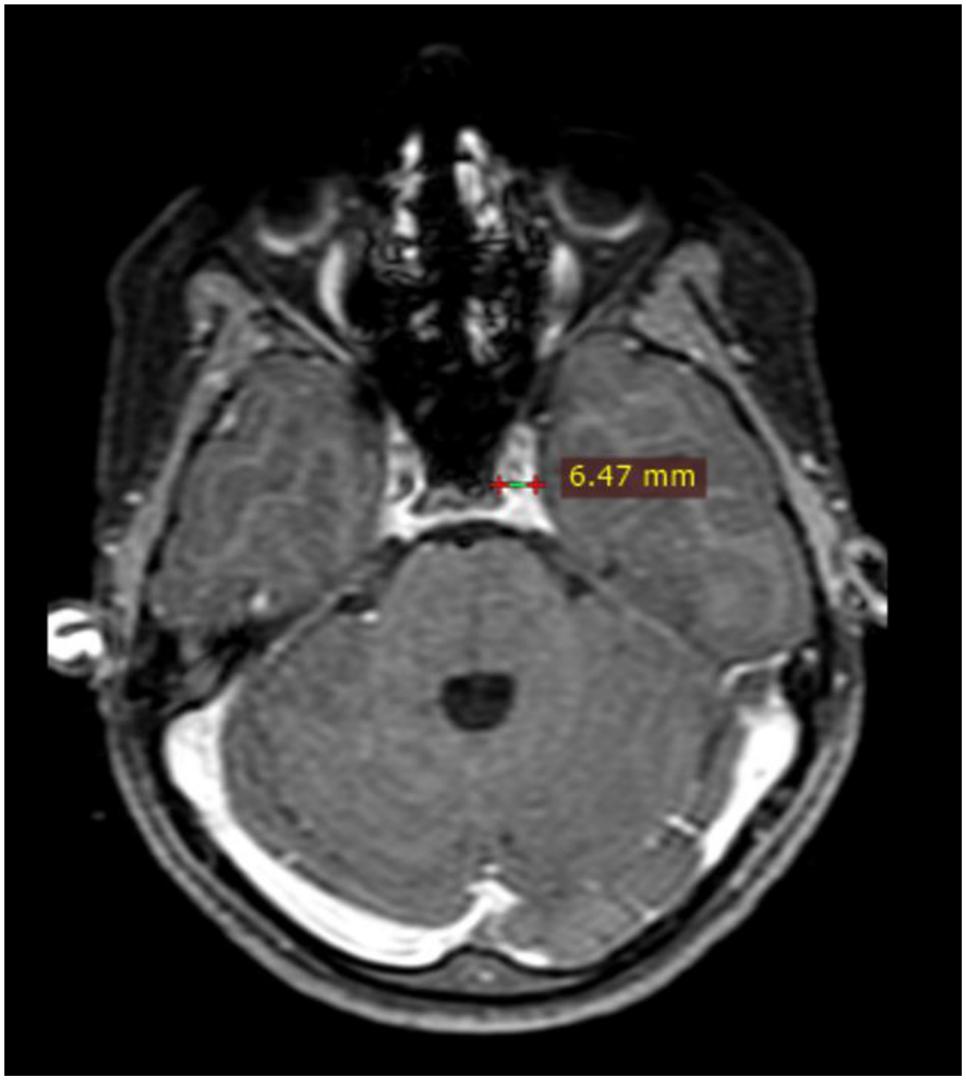

Fig. 2. Axial post contrast fat saturated T1W image shows: Measurement of the cavernous sinus diameter on the left.

various imaging parameters in the MRI evaluation of cavernous sinus thrombosis on contrast enhanced MRI as there is sparse literature concerning these, except for a few case reports.

Fig. 1 denotes a diagrammatic representation of the cavernous sinus anatomy.

2. Materials and methods

Retrospective review of the PACS and electronic medical records of patients who underwent imaging (Contrast enhanced MRI performed on 1.5 T MRI scanner, Achieva; Philips Medical Systems) from January 2016 through July 2019 was performed. Patients were first identified in the imaging database by searching for the keywords “cavernous sinus thrombosis” and “cavernous sinus thrombophlebitis”.

The criteria for inclusion in the cavernous sinus thrombosis group were a clinical suspicion of CST and contrast enhanced MRI of the brain with sagittal, axial and coronal planes (T2, FLAIR and post contrast T1W 3D sequence). The particulars of the sequences are as under:

- T1-weighted turbo spin-echo imaging (760/15 [repetition time msec/echo time msec (TR/TE)])
- T2-weighted turbo spin-echo imaging (TR/TE = 8412/100)
- Short inversion time inversion- recovery or STIR (TR/TE = 6961/80)
- Intravenous Contrast- Gadolinium based contrast agents: Gadopentetate dimeglumine (0.1 mmol/kg at a rate of 2–3.5 ml/second, employing hand injection technique)
- Post contrast scan: T1W 3D sequence obtained 3–5 min after contrast administration.

A total of 7 cases were identified.

Control subjects were selected from the same imaging time period and were matched for age and sex. The control subjects were patients who underwent contrast-enhanced MRI for clinical symptoms of headache or epilepsy, but there was no clinical suspicion of cavernous sinus thrombosis, whatsoever.

7 such individuals comprised the control group.

Patients with known malignancies involving the pituitary/sinonasal

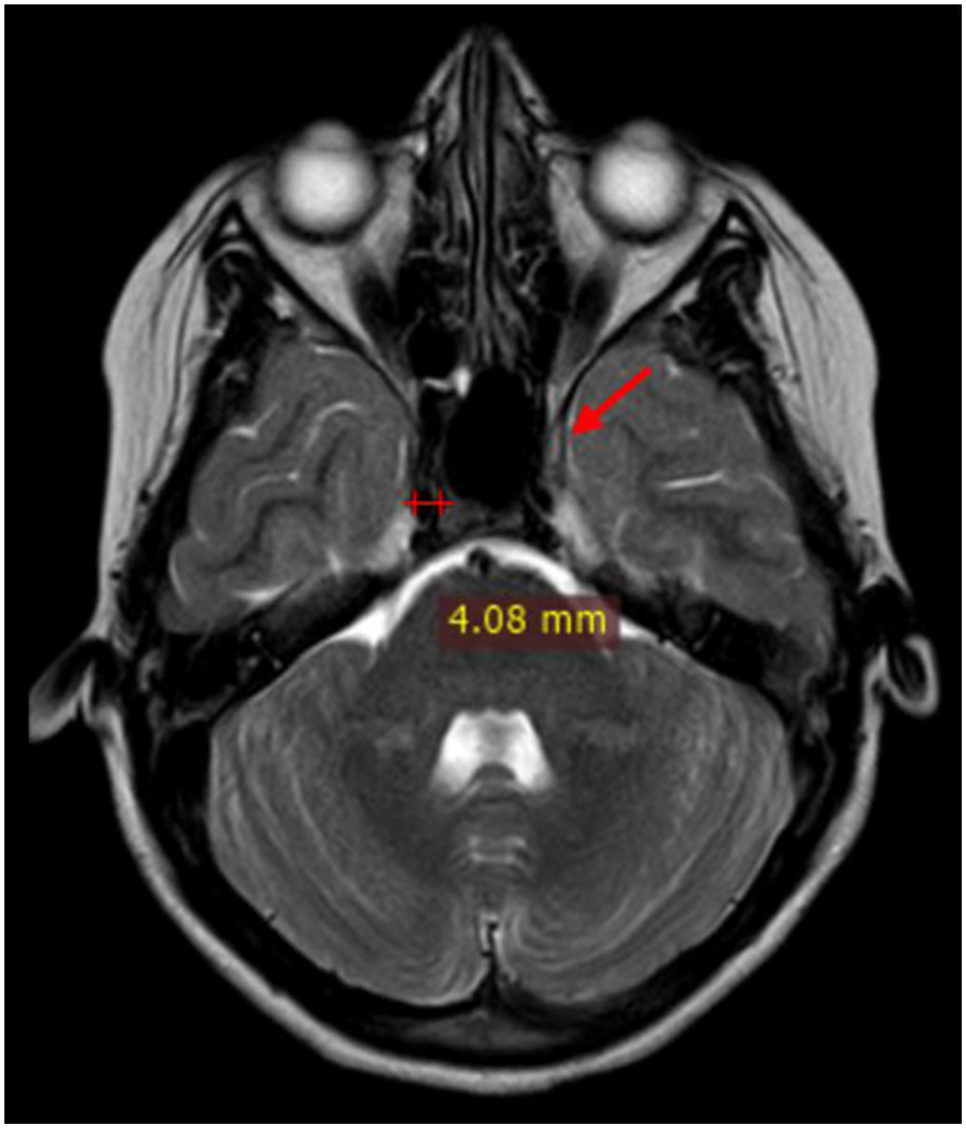

Fig. 3. Axial T2WI shows: Measurement of diameter of right cavernous ICA flow void and red arrow denoting the normal concave lateral wall of the left cavernous sinus.

/spheno-clival regions were excluded from the study.

A retrospective analysis of the patients' requisition forms was made and patient details were sought. A thorough clinical history, examination and treatment follow up of the patients were obtained, as summarised in Table 1.

Two radiologists with an experience of 20 and 7 years, respectively, reviewed the MRI studies. The following parameters were assessed bilaterally for evidence of CST. (Table 2)

Maximum diameter of the cavernous sinus on axial images was recorded **(**Fig. 2**).** Diameter of the flow void of the cavernous segment of ICA was measured on axial images and loss of flow void on plain MRI was considered as thrombosis **(**Fig. 3**).** The diameter of the superior ophthalmic vein was measured on coronal scans, on a section nearest to the rear of the globe **(**Fig. 4**).** Loss of flow void on plain MRI or non-opacification on contrast images was considered as a sign of thrombosis.

Qualitative parameters were also evaluated by both the reviewing radiologists.

Sinus walls were assessed on axial and coronal sections to look for bulging or convex walls. Abnormal signal intensity was seen on plain MRI, while post contrast images were analysed for any heterogeneity or filling defect within the sinus along with presence of abnormal dural enhancement along its lateral wall.

Extent of proptosis was measured on axial scans and a globe protrusion > 21 mm anterior to the interzygomatic line on axial images, at the level of lens, was considered to be positive. [17] **(**Fig. 5**).** Orbital apex, intra, extraconal and preseptal compartments were evaluated for loss of normal fat signal (or presence of abnormal signal intensity) on

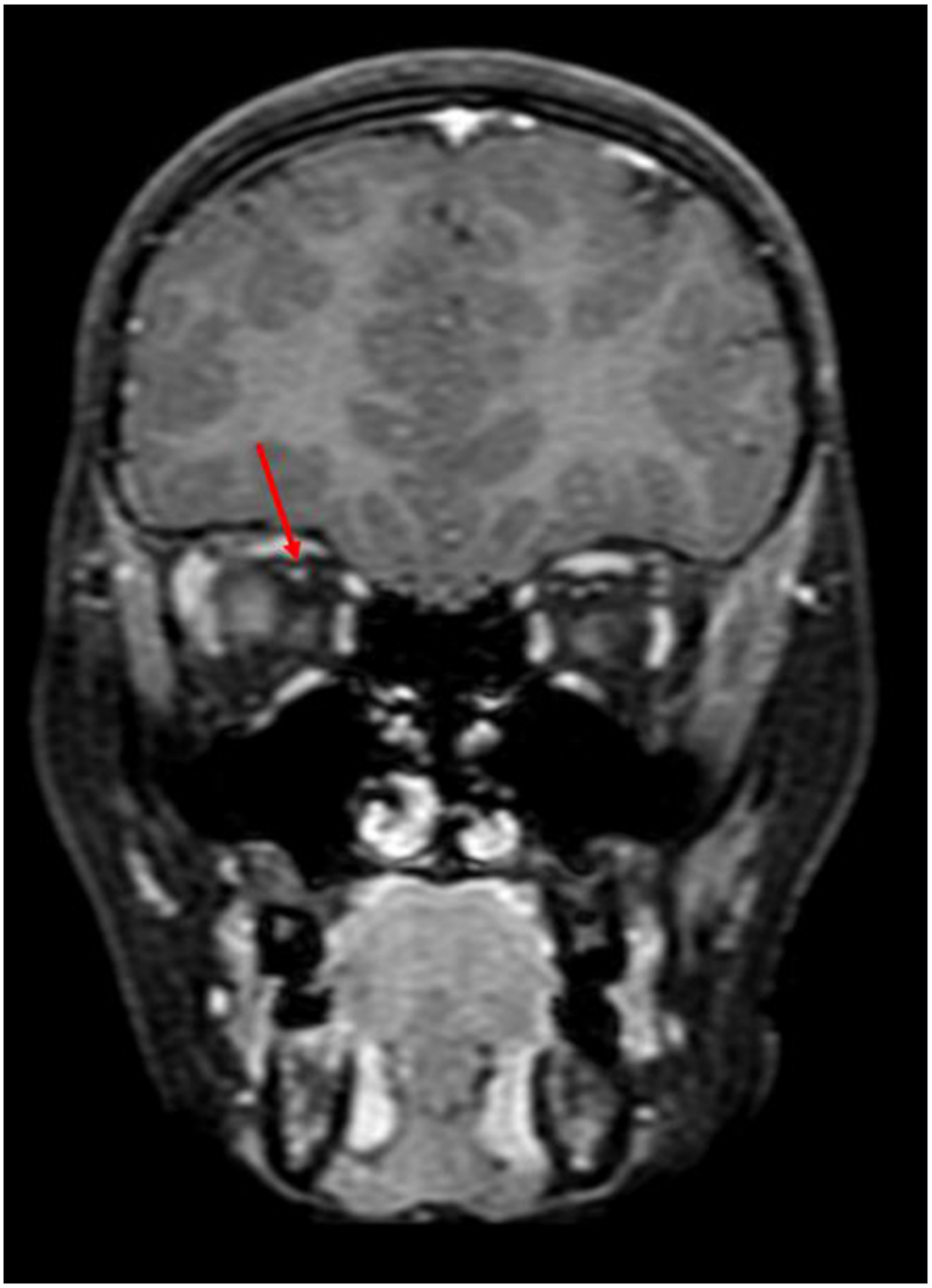

Fig. 4. Coronal post contrast fat saturated T1W image shows: Level of measurement of SOV diameter on the right (red arrow).

plain MRI, or presence of any enhancement on post contrast images.

Other features like thrombosis of IJV and other dural venous sinus, involvement of the surrounding regions including the sphenoid, petrous apex, pituitary gland, and intraparenchymal abnormality were also evaluated.

2.1. Statistical analysis

For group comparisons, categoric variables were compared using a chi-square test or Fisher exact-test, as appropriate. For continuous variables, the Student *t* test was used. All data were analyzed using two tailed tests and a p value of < 0.05 was considered significant. Inter observer agreement between the readers was assessed using Cronbach's alpha test. An α value of ≥ 0.9 indicated excellent consistency; 0.8-0.9, good consistency; 0.7-0.8, acceptable consistency, 0.6-0.7, questionable consistency, 0.5-0.6, poor consistency and ≤ 0.5 unacceptable consistency. A cut point for the discriminatory variables was estimated using receiver operating characteristic (ROC) curves. All statistical analysis was performed using IBM SPSS software (version 22).

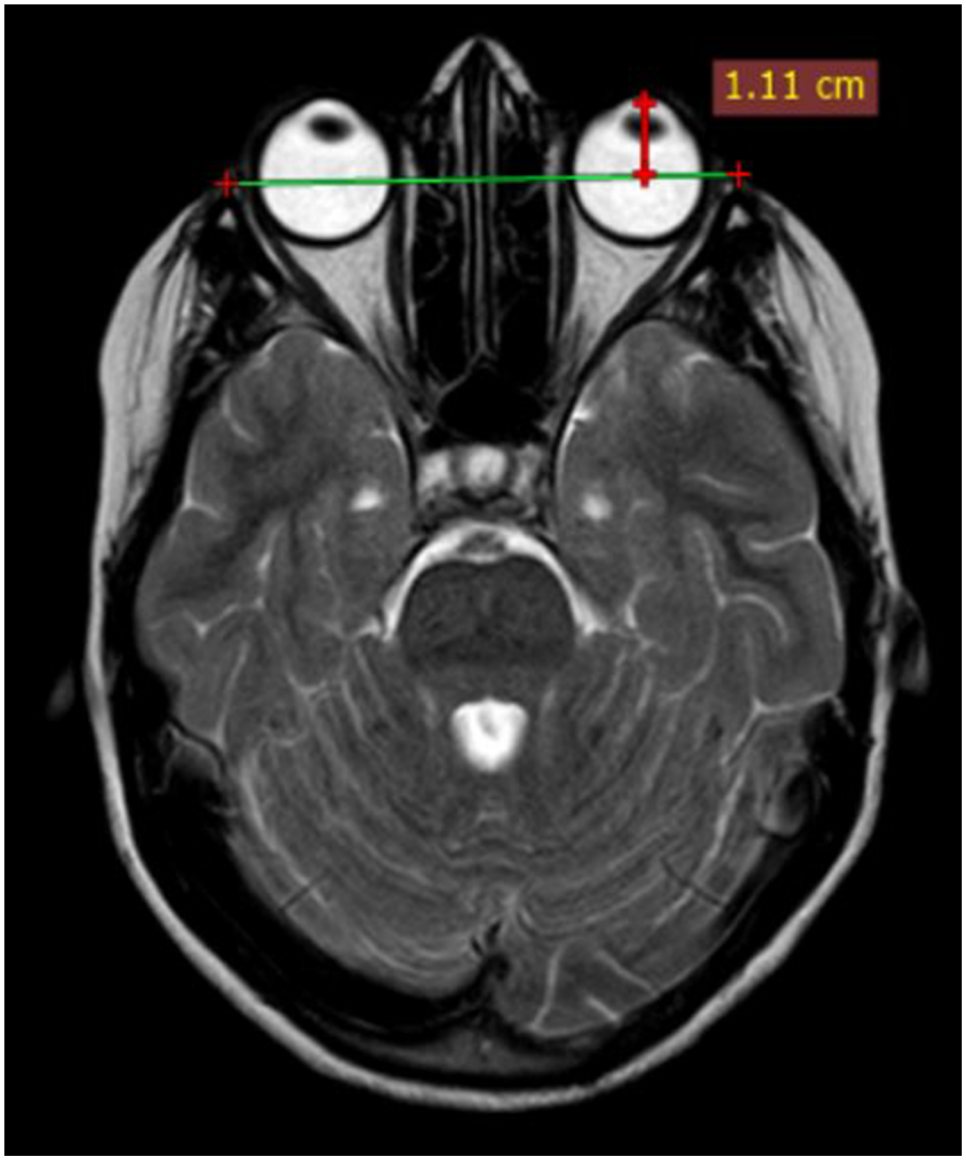

Fig. 5. Axial T2WI shows: Proptosis as measured anterior to the interzygomatic line on the left.

Table 3
Qualitative parameters in CST group.

	Lateral wall	Signal intensity	Filling defect	Dural enhancement along lateral wall	Orbital apex involvement	Proptosis	Preseptal involvement
1.	Convex	Abnormal	–	+	+	–	–
2.	Straight	Abnormal	–	+	+	–	–
3.	Convex	Abnormal	+	+	–	–	–
4.	Convex	Normal	+	+	–	–	–
5.	Convex	Normal	+	+	+	+	–
6.	Convex	Abnormal	+	+	+	–	+
7.	Convex	Abnormal	+	+	–	–	+
8.	Convex	Abnormal	–	+	+	+	+
9.	Convex	Abnormal	–	+	+	+	+

Table 3 denotes the results of the qualitative parameters assessed in CST group.

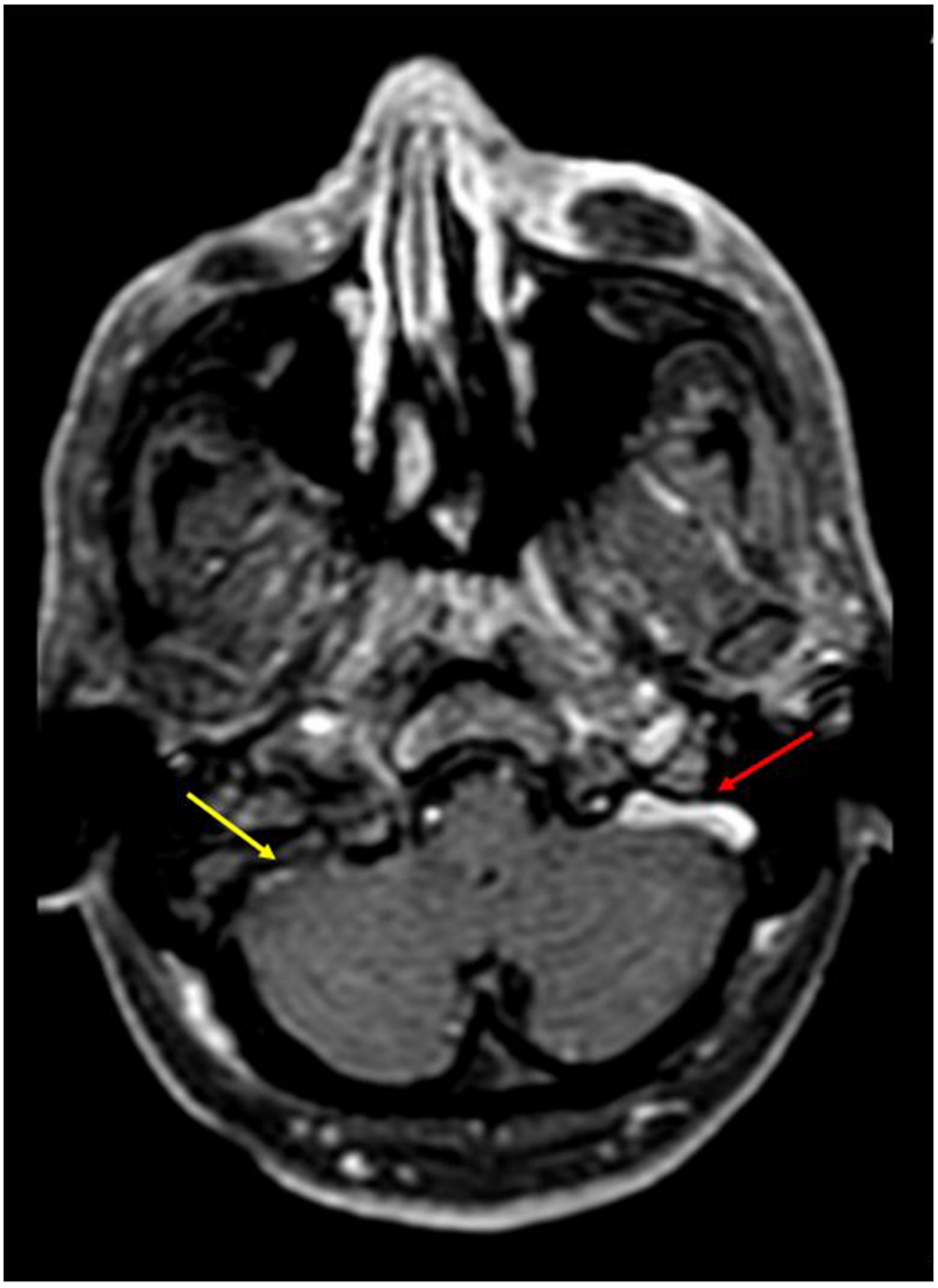

Fig. 6. Axial post contrast T1W image shows: Thrombosed right sigmoid sinus and IJV (yellow arrow), in comparison to the normal left side (red arrow).

Table 4
Quantitative parameters in CST group v/s control group.

	Group	N	Mean	Std. Deviation	p value
Size of cavernous sinus	Cases	9	9.14 mm	0.565 mm	.002
	Controls	14	6.58 mm	0.541 mm	
Cavernous ICA status	Cases	9	3.533 mm	.9042 mm	.001
	Controls	14	4.657 mm	.4433 mm	
SOV	Cases	9	3.800 mm	1.7965 mm	.000
	Controls	14	1.194 mm	.1165 mm	

Table 4 denotes the comparison of results and the statistical significance in the quantitative parameters in both the groups.

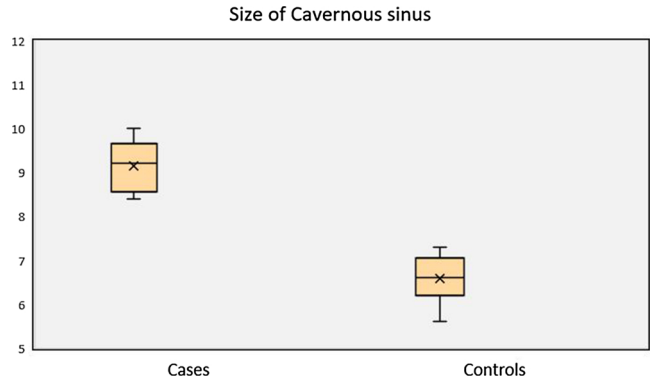

Fig. 7. Box plot showing: Statistically significant difference in average size of cavernous sinus in patients with CST (Mean ± SD; 9.1 mm ± 0.56 mm) and control subjects (6.5 mm ± 0.54 mm).

3. Results

3.1. Cases

There were 7 patients with an MRI diagnosis of cavernous sinus thrombosis and 7 control subjects. Of these 7 cases, 4 were men (57.1 %) and 3 were women (42.9 %); they ranged in age from 10 to 73 years old (mean age, 34.29 years, SD ± 20.0)

14 cavernous sinuses were analysed on MRI in 7 patients. Unilateral involvement was seen in 5 patients (left in four, right in one) while bilateral involvement was noted in 2 patients, comprising a total of 9 affected cavernous sinuses.

In the 9 cavernous sinuses which were affected in the cases group, mean cavernous sinus diameter was 9.14 mm on axial scans (SD ± 0.56 mm), mean cavernous ICA diameter was 3.5 mm (SD ± 0.9 mm), mean SOV diameter was 3.8 mm (SD ± 1.79 mm)

Qualitative parameters as assessed, are summarised in Table 3.

8 out of 9 affected sinuses (88 %) showed bulging or convex margins, while one (12 %) showed straight margins, instead of normal concave walls.

77.7 % (7 out of 9 sinuses) showed altered signal intensity on plain MRI, while, 5 sinuses (55.5 %) showed filling defects on post contrast images.

All sinuses that were affected on MRI (100 %), showed dural enhancement along their lateral walls.

3 sinuses (33 %) showed thrombosis of the Superior Ophthalmic Vein.

There was orbital involvement in 7 sinuses (77.7 %), in the form of involvement of the orbital apex in 6 patients (66.6 % of affected sinuses), preseptal compartment in 4 (44.4 %), intraconal compartment in 3 patients (33.3 %), extraconal compartment in one patient and proptosis in 3 (33 % of affected sinuses).

Intraparenchymal abnormalities were noted in 2 patients, where one had an abscess in temporal lobe, while the other had a small subdural collection with overlying meningeal enhancement.

3.2. Additional findings

Dural enhancement was seen to extend along the pituitary (one patient), the petrous apex, sphenoid and clivus (one patient) and along prepontine, premedullary and perimesencephalic cistern(one patient). IJV was seen to be thrombosed in 2 patients while sigmoid sinus showed evidence of thrombosis in one. **(**Fig. 6**)** A frontal subperiosteal abscess was seen in one patient, while enhancing collections over the maxillary bone were seen in another patient.

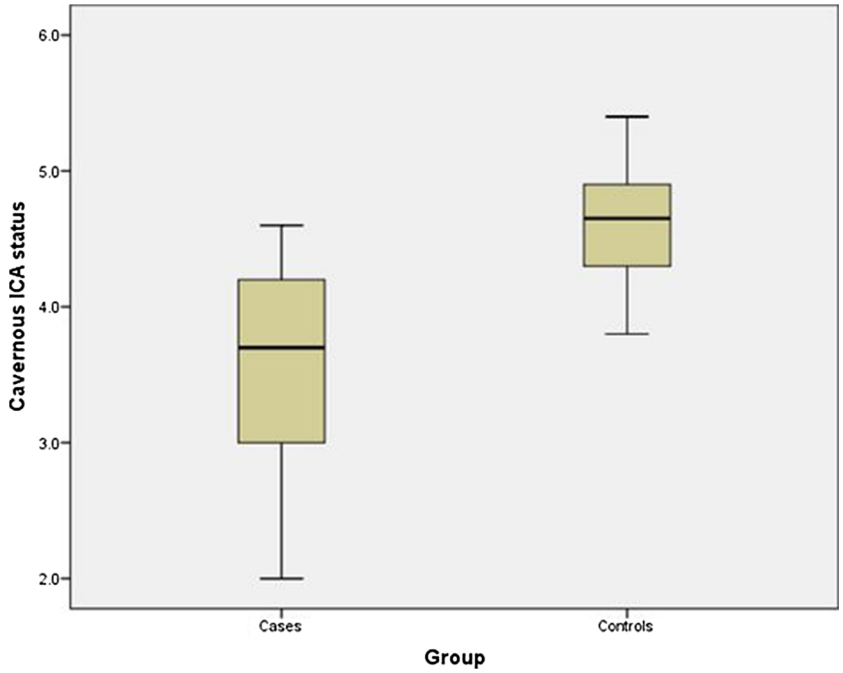

Fig. 8. Box plot showing: Statistically significant difference in average diameter of Cavernous ICA segment in patients with CST (Mean ± SD; 3.5 mm ± 0.9 mm) and control subjects (4.6 mm ± 0.44 mm).

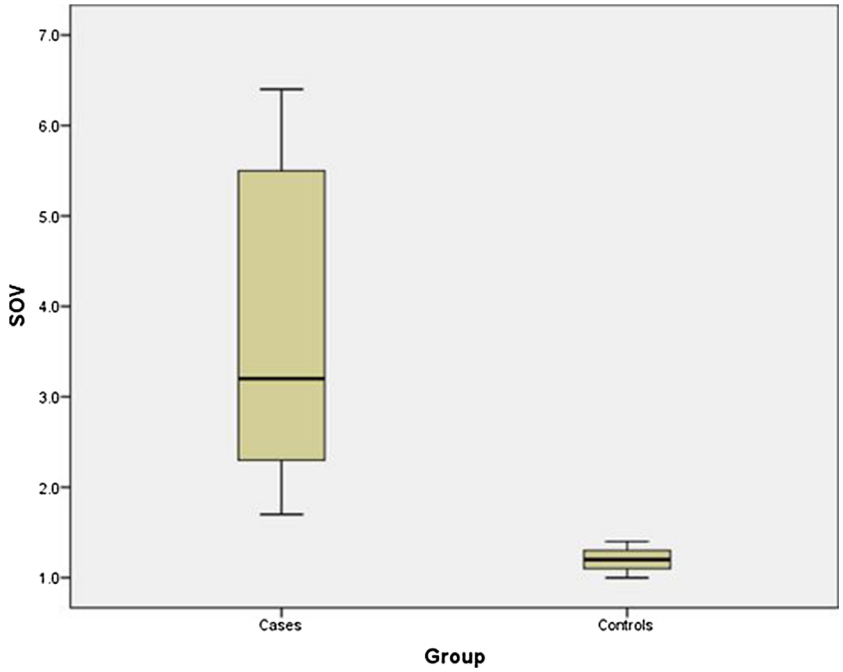

Fig. 9. Box plot showing: Statistically significant difference in average diameter of Superior Ophthalmic Vein in patients with CST (Mean ± SD; 3.8 mm ± 1.79 mm) and control subjects (1.19 mm ± 0.11 mm).

3.3. Controls

In the control group of 7 subjects, there were 4 men (57 %) and 3 women (43 %); the subjects ranged in age from 8 to 72 years, (mean age, 35.7 years, SD ± 22.4 years).

The mean cavernous sinus diameter was 6.58 mm on axial scans (SD ± 0.54 mm), mean cavernous ICA diameter was 4.6 mm (SD ± 0.44 mm), mean SOV diameter was 1.1 mm (SD ± 0.11 mm).

All the cavernous sinuses showed concave margins on axial scans with no filling defect or heterogeneity on the post contrast images.

ICA and SOVs showed normal flow voids in all patients.

Orbital apex, intra and extraconal orbital compartments showed normal signal intensity fat on plain MRI with no abnormal signal intensity or enhancement on post contrast images.

There were no significant intra or extraparenchymal abnormality noted in any of these subjects.

The difference in the cavernous sinus diameter for the cavernous sinus thrombosis group versus the control group was statistically significant ($p < 0.01$) with excellent inter-observer reliability (α-0.998). Similarly, the difference in cavernous ICA flow void diameters between the two groups was statistically significant ($p < 0.01$) with excellent inter-observer reliability (α-0.982). Also, the diameter of the SOV flow void was significantly different in the CST and the control group ($p < 0.01$) with an excellent inter-observer reliability (α-0.996). **(**Table 4, Figs. 7–9**)**

Bulging lateral walls were seen in 8 out of 9 affected sinuses, while none of the individuals in the control group had bulging or convex sinus walls. Orbital involvement was seen in association to the thrombosed sinus in 7 out of 9 cases, while appearing completely normal in control group.

Of all the qualitatively assessed variables; features including bulging lateral walls, abnormal dural enhancement along lateral wall, altered signal intensity on plain scan and filling defects on post contrast scans showed excellent inter observer agreement (α > 0.9), while involvement of the orbital apex and the presence of proptosis showed good interobserver agreement (α:0.8-0.9).

4. Discussion

Cavernous sinus thrombosis can have septic as well as aseptic causes, septic being much more common. It most often occurs as a complication of bacterial or fungal sepsis in the paranasal sinuses, the face, the orbits, and the skull base. More commonly it results from local spread, often from valveless facial and ophthalmic veins, more severely affecting diabetic and immunocompromised patients, who are on steroid use or on chemotherapy.

Aseptic causes including trauma and surgery may lead to this vascular complication.

Patients most commonly complain of fever, headache (50%–90%), and orbital symptoms like periorbital swelling and pain, vision changes, such as photophobia, diplopia and loss of vision.

In our study, all 7 cases had an infectious or a septic cause attributable to cavernous sinus thrombosis. These presented with symptoms of fever and headache, out of which 6 cases had orbit related complaints, including diplopia which was a clinical feature in all these patients.

None of the cases had an aspetic cause attributable to the thrombosis.

The optimal diagnostic test is neuroimaging with either contrast-enhanced computed tomography (CT) or magnetic resonance imaging (MRI).

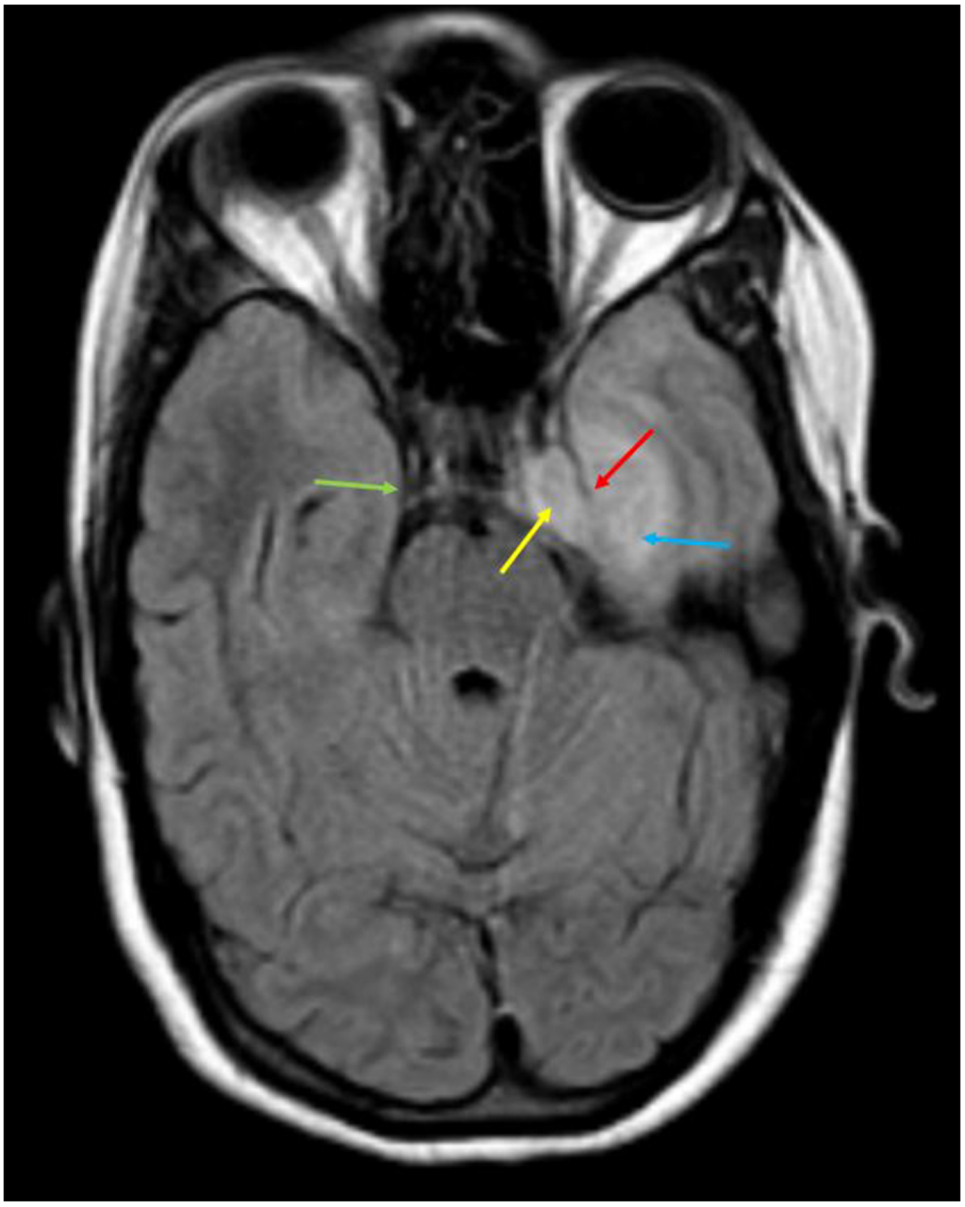

Fig. 10. Axial FLAIR image shows: Expanded left cavernous sinus with hyperintense soft tissue within it (yellow arrow), with bulging lateral wall (red arrow); in comparison to the concave wall of the normal right cavernous sinus (green arrow); hyperintensity in the left medial temporal lobe (blue arrow).

There are certain direct and indirect imaging signs of cavernous sinus thrombosis, with coronal scans proving extremely informative [7–10].

Direct signs, including changes in signal intensity, size and contour (or configuration) of the cavernous sinus are extremely useful signs [18].

Cavernous sinus on imaging shows concave lateral walls on coronal images [19].

Enlargement and expansion of the sinuses with bulging or convex lateral walls on coronal scans has been considered to be an important indicator of cavernous sinus lesions [20,22]. In our study, transverse diameter in controls was reported as 6.58 mm, while thrombosed sinuses had an average transverse diameter of 9.14 mm, and the difference was statistically significant ($p < 0.001$). A cut-off value of cavernous sinus diameter $\geq$ 10 mm had a sensitivity of 77.8 %, specificity of 92.8 %, Positive Predictive Value (PPV) of 87.5 %, NPV of 86.6 % and an accuracy of 86.96 % in diagnosing CST. This is significantly higher than the normally reported transverse diameter of 5–7 mm and vertical diameter of 5–8 mm [19].

In a study conducted by Mee Young et al. [20] in 1994, about 27 patients were studied to evaluate and classify cavernous sinus lesions using CT as well as MRI. Diffuse convex bulging of the lateral wall of cavernous sinus was the most frequent radiological finding, indicative of a cavernous sinus lesion.

Ahmadi et al. [10] in 1988, concluded that bulging of the lateral wall was the most sensitive indicator of pathologic involvement of cavernous sinus, because, irrespective of the cause, it led to volume expansion of the involved cavernous sinus.

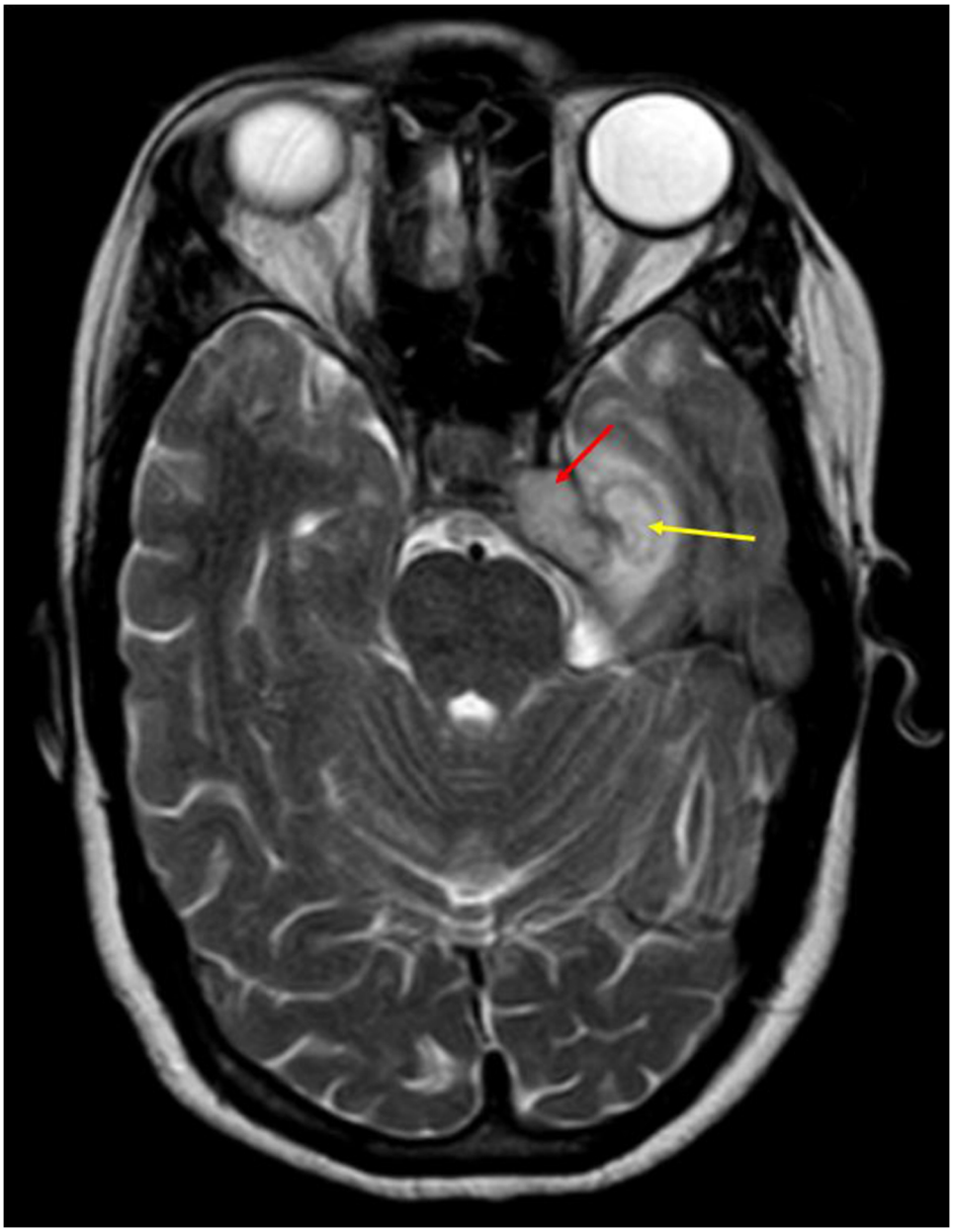

Fig. 11. Axial T2WI shows: Hyperintense soft tissue in left cavernous sinus (red arrow); with an abscess in left medial temporal lobe (yellow arrow) compressing ipsilateral basal cistern.

Our study is in concordance with these and showed convex lateral walls of the sinus to be present in all 9 affected sinuses. On the other hand, the control group had normal (or concave) walls. **(**Figs. 10 and 11**)**

Scotti et al. [21] in 1986, conducted a study on MR imaging of cavernous sinus involvement by pituitary adenomas and found that the most sensitive MR sign of cavernous sinus invasion/ involvement was an asymmetry between the two sides. In our study too, 5 patients that showed asymmetric unilateral CS involvement in the form of expansion and abnormal signal intensity.

Cavernous sinus, being a septated venous space containing flowing blood, produces negligible signal intensity on plain MRI sequences [20].

On post contrast images, normal cavernous sinuses show intense enhancement of the slower flowing venous blood.

In our study, 7 out of 9 affected cavernous sinuses showed altered signal intensity of the cavernous sinus that appeared heterogeneously hypointense to grey matter on T2WI in 5 sinuses, and isointense in 2 sinuses. In 4 of these 7 sinuses, the inflammatory soft tissue showed heterogenous enhancement on post contrast images, while in the other 3, the soft tissue appeared as a filling defect on post contrast images. **(**Figs. 10–13**)**

The other two patients did not show any altered signal intensity on plain MRI but showed multiple irregular filling defects on post contrast images which were likely due to intrasinus thrombi [7–9] **(**Fig. 12**)**.

The control group on the other hand showed normal signal intensity

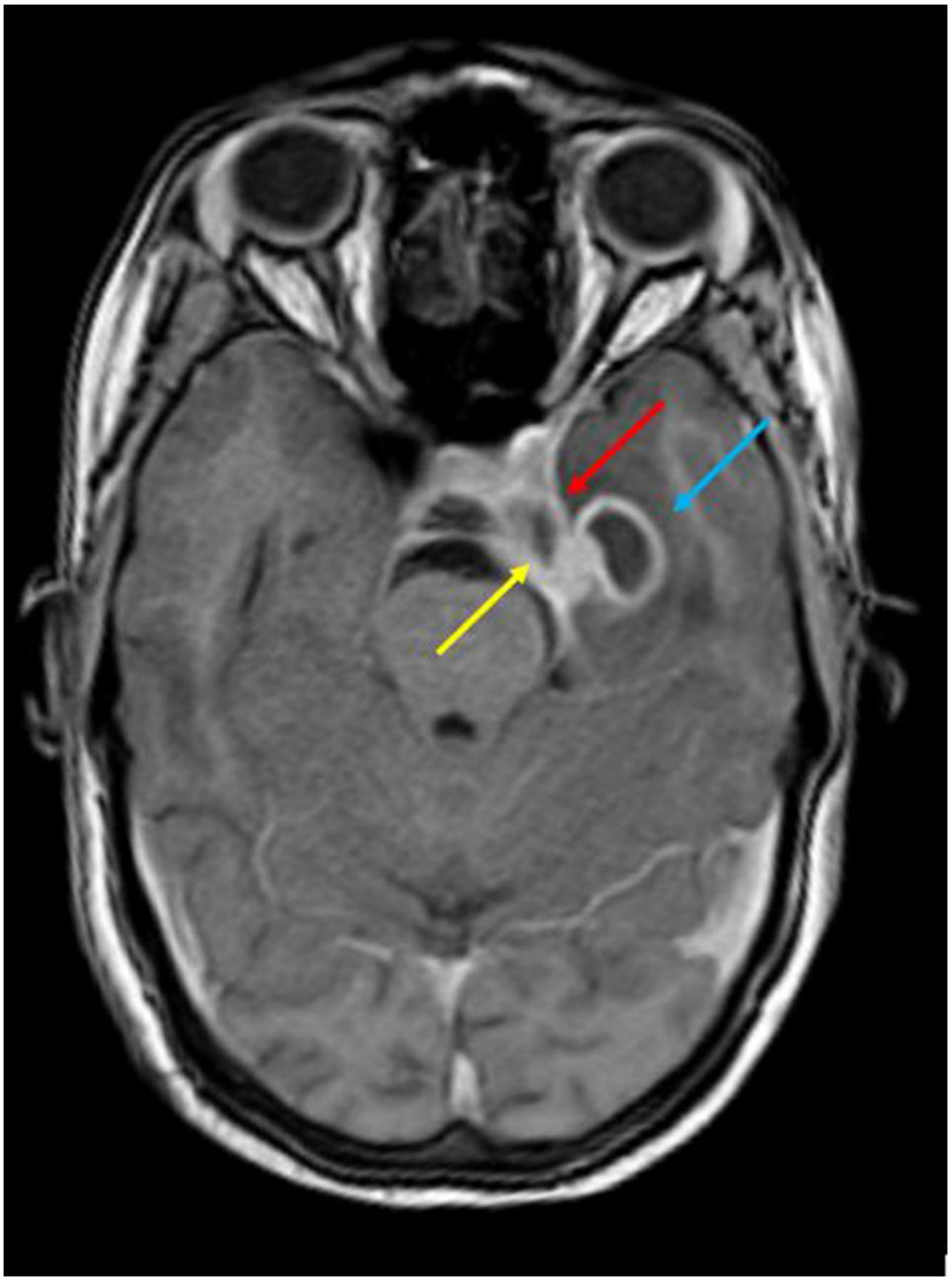

Fig. 12. Axial T1 post contrast image shows: Bulging wall of the left Cavernous sinus with abnormal dural enhancement (red arrow); Filling defect in the left cavernous sinus (yellow arrow); ring enhancing abscess in left temporal lobe (blue arrow).

and smooth intense enhancement of the cavernous sinuses, which was statistically significant (p value < 0.001)

Horizontal segment of the ICA is an important component that traverses the cavernous sinus and can be significantly affected in a number of cavernous sinus lesions.

It appears as a normal flow void on cross sectional imaging, with a reported diameter of about 5 mm [23].

In the study conducted by Mee young et al [20] while evaluating cavernous sinus lesions on CT and MRI, in 1995, carotid artery encasement (or displacement) was reported to be the second most frequent radiologic finding in cavernous sinus lesions after convex bulging walls.

In a case report of septic thrombosis of cavernous sinus by Jisun

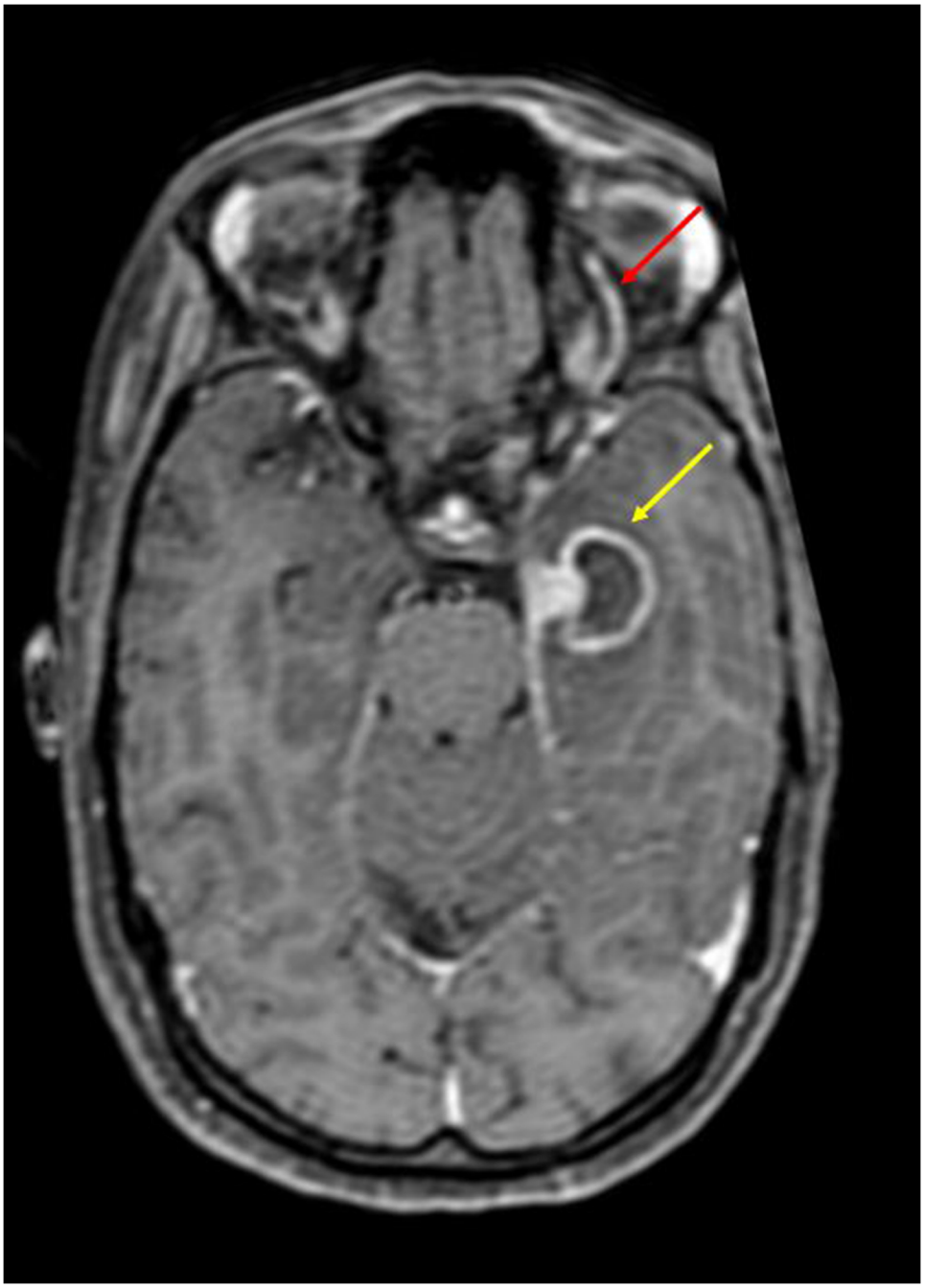

Fig. 13. Axial post contrast fat saturated T1W image shows: Dilated left superior ophthalmic vein (red arrow); ring enhancing abscess in left temporal lobe (yellow arrow).

Hwang in 2015, there was narrowing of the flow void of the cavernous ICA, which was considered as a sign of compression of ICA [18].

In our study, mean ICA flow void diameter was 3.5 mm, as compared to controls, where it measured 4.6 mm which was significantly different (p value < 0.05). A cut-off value of ICA flow void diameter $\leq$ 4.2 mm showed a sensitivity of 77.7 %, specificity of 85.8 %, PPV of 77.7 %, NPV of 85.7 % and an accuracy of 82.61 % in diagnosing CST. **(**Fig. 14**)**

This was significantly lower in comparison to the normally reported diameter of 5 mm on transverse scans [23].

None of the affected cases showed thrombosis of ICA or loss of flow void.

Amongst the various venous connections of the cavernous sinus, the superior and inferior ophthalmic veins are important tributaries that

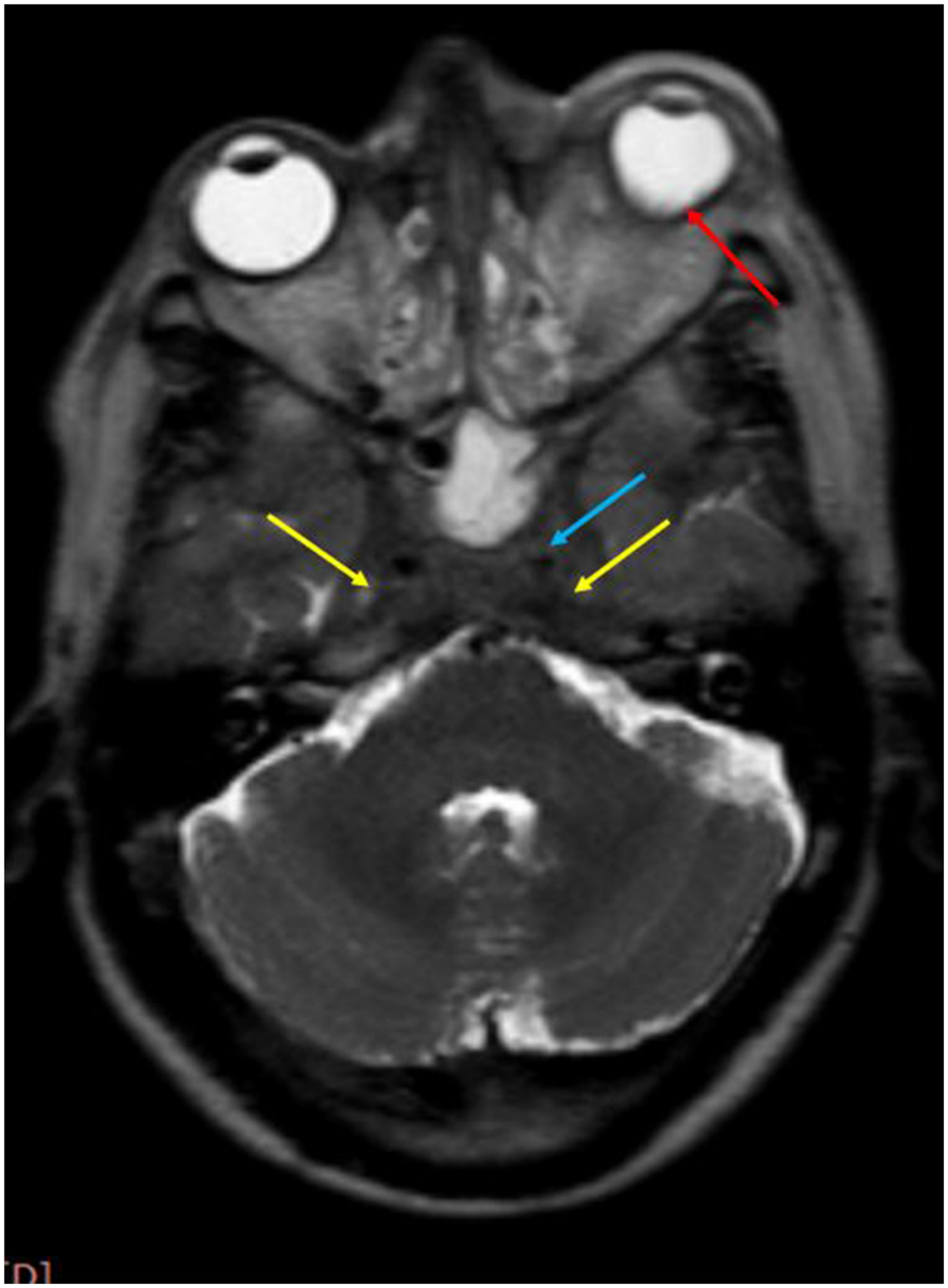

Fig. 14. Axial T2WI shows: Hypointense soft tissue filling and expanding both cavernous sinuses (yellow arrows); Compressed flow void of left cavernous ICA (blue arrow); Left sided staphyloma (red arrow).

drain into the cavernous sinus. When there is thrombosis of the sinus, there is impaired drainage of blood from the superior ophthalmic vein, thus leading to its engorgement.

Dilatation (and /or subsequent thrombosis) of the superior ophthalmic vein, is thus, an indirect sign of cavernous sinus thrombosis [1,19,20].

The normal diameter of Superior ophthalmic vein ranges from 1 to 2.9 mm as measured on coronal scans [24].

SOV dilatation is a frequently found in cases of CST and was found in all 4 cases reported by Jisun Hwang in 2015 [18].

In a study conducted by Weir et al. [25] in 2002, one hundred and sixteen cases of enlarged SOV were analysed by CT and MRI and the diameter of the enlarged vein was reported as 3.5 − 7 mm. Carotid cavernous fistula was diagnosed as the cause in 92 cases while CST was seen in only one.

In our study, the SOV dilatation was seen in the case group (mean diameter 3.8 mm), compared to the control group (1.19 mm) which was statistically significant. (p value < 0.001) **[**Fig. 13**]**. A cut off value of

Fig. 15. Axial FLAIR shows: Left sided staphyloma (yellow arrow) and proptosis; with hyperintensity in the left preseptal compartment (red arrow).

SOV diameter of ≥ 2.9 mm was considered to be 100 % sensitive, specific and accurate in predicting CST, which is in concordance with the normal reported upper limit of 2.9 mm on coronal scan [24].

SOV, however was found to be thrombosed in only 3 of 9 cases. **(**Figs. 16 and 17**)**

Apart from SOV dilatation, other indirect signs of CST include exophthalmos and increased dural enhancement along the lateral border of Cavernous sinus and ipsilateral tentorium [20].

In our study, exophthalmos was seen in 2 cases, while abnormal dural enhancement along the lateral wall was seen in all cases. **(**Figs. 14 and 18**)**

Thus, of all the quantitative variables evaluated in the study, SOV dilatation (of ≥ 2.9 mm) was considered to be the most sensitive and specific marker of CST. Enlargement of the cavernous sinus with a diameter of ≥ 10 mm had a relatively high specificity of 92.8 %, while a compressed ICA flow void (measuring ≤ 4.2 mm) had a good accuracy of about 82.6 % (but least of the three) in diagnosing this condition.

Orbital involvement is a frequent association in cavernous sinus thrombosis, with most of the patients presenting with eye related symptoms.

In our study, 7 out of 9 sinuses had orbital apex involvement, either in the form of altered signal intensity tissue at the apex (in 6) or as abnormal enhancement in the region (3 sinuses**).** **(**Figs. 14–18, Fig. 6**).** Preseptal involvement, however was noted in 4 patients. **(**Fig. 15**)**

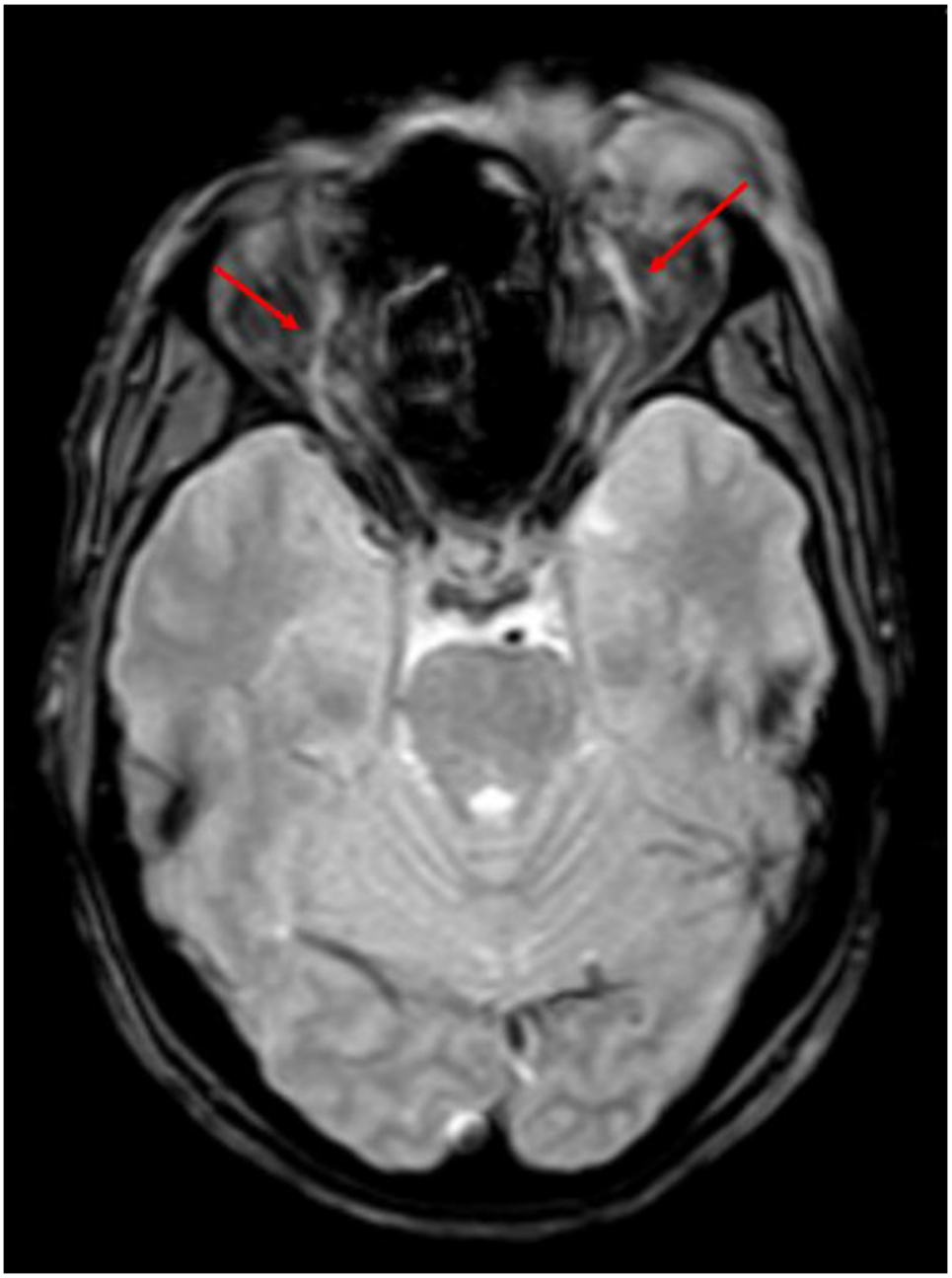

Fig. 16. Axial T2W FFE image shows: Dilated bilateral SOVs with loss of flow void suggestive of thrombosis (red arrows).

Intraparenchymal abnormalities can accompany CST in many patients, either as a primary source of infection or a spread from a contiguous/venous source. This was seen in one patient in our study, who was a known case of pulmonary TB and presented with altered sensorium and diplopia. Imaging revealed a peripherally enhancing abscess in temporal lobe along with overlying meningeal enhancement, which was seen to extend along ipsilateral basal cisterns and along tentorium. **(**Fig. 12**)**

5. Limitations

Main limitations of this study are its retrospective nature and small number of subjects owing to its rare occurrence. Further the readers were not blinded to clinical diagnosis which could have resulted in bias.

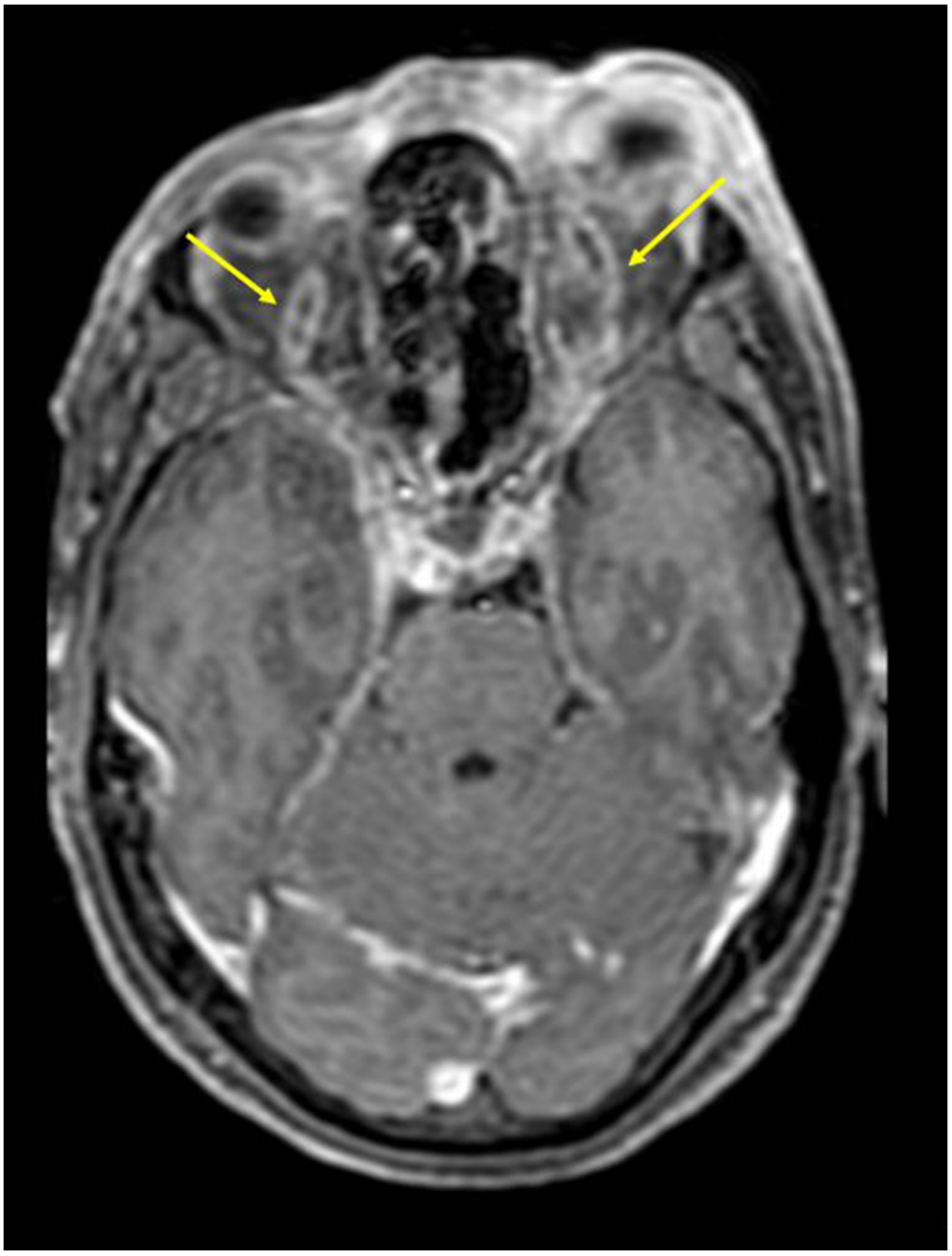

Fig. 17. Axial post contrast fat saturated T1W images show: Dilated and thrombosed bilateral superior ophthalmic veins (yellow arrows).

6. Conclusions

The diagnosis of cavernous sinus thrombosis is usually predicted clinically, but one should not only be aware of its various imaging findings, but, should also be familiar with certain proposed parameters as MRI is commonly carried out in such patients to see the extent of disease, associated complications and to establish the etiology of thrombosis. Qualitative parameters like bulging lateral walls of the sinus, abnormal dural enhancement of the lateral wall, abnormal signal intensity of the sinus and presence of filling defects on post contrast scans are useful indicators of predicting cavernous sinus thrombosis. All the three described quantitative variables, including an enlarged cavernous sinus with a dimeter of $\geq$ 10 mm, a dilated SOV with a diameter of $\geq$ 2.9 mm and a compressed ICA flow void with a diameter of $\leq$ 4.2 mm are good predictors of cavernous sinus thrombosis with SOV dilatation having the maximum diagnostic accuracy, sensitivity and specificity followed by an enlarged cavernous sinus size and compressed ICA flow void respectively. Thus, these objective criteria can help recognise this potentially fatal abnormality at an early stage.

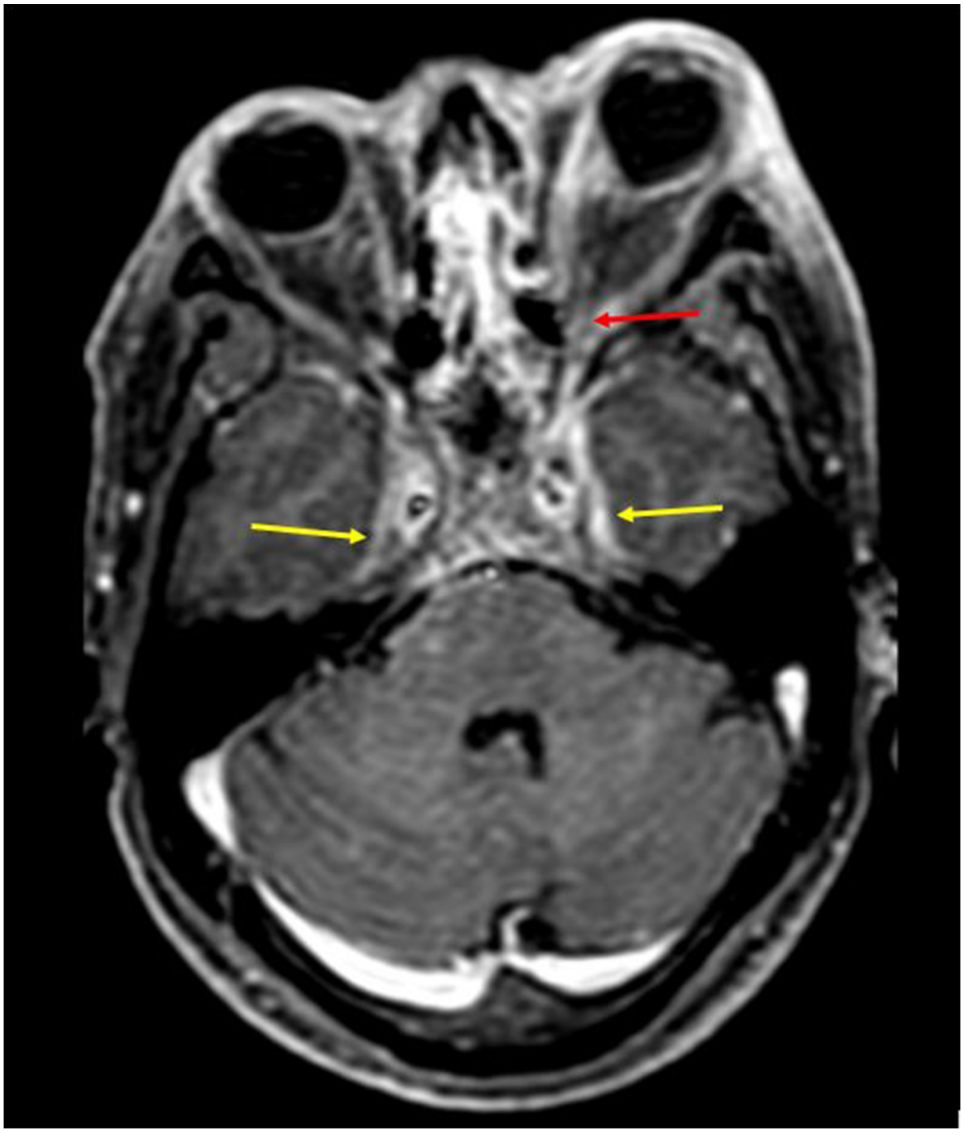

Fig. 18. Axial post contrast T1W image shows: Abnormal dural enhancement along lateral walls of both cavernous sinuses (yellow arrows); with enhancement extending up to the left orbital apex (red arrow).

Funding

This research did not receive any specific grant from funding agencies in the public, commercial, or not-for-profit sectors.

CRediT authorship contribution statement

Harsimran Bhatia: Conceptualization, Data curation, Methodology, Formal analysis, Writing - original draft. **Ravinder Kaur:** Investigation, Methodology, Writing - review & editing. **Raveena Bedi:** Software, Validation, Visualization, Supervision.

Declaration of Competing Interest

This is to state that the authors and the authors' institute have no conflict of interest,

References

[1] M.C. Plewa, P. Tadi, M. Gupta, Cavernous Sinus Thrombosis, StatPearls Publishing, StatPearls. Treasure Island (FL), 2019.
[2] T.J.H. Matthew, A. Hussein, Atypical cavernous sinus thrombosis: a diagnosis challenge and dilemma, Cureus 10 (12) (2018), https://doi.org/10.7759/cureus.3685.
[3] A.S. Eltayeb, M.A. Karrar, E.I. Elbeshir, Orbital subperiosteal abscess associated with mandibular wisdom tooth infection: a case report, J. Maxillofac. Oral Surg. 18 (1) (2019) 30–33, https://doi.org/10.7759/cureus.3685.
[4] C. Dolapsakis, E. Kranidioti, S. Katsila, M. Samarkos, Cavernous sinus thrombosis due to ipsilateral sphenoid sinusitis, BMJ Case Rep. 12 (1) (2019), https://doi.org/10.1136/bcr-2018-227302.
[5] M.C. Chen, Y.H. Ho, P.N. Chong, J.H. Chen, A rare case of septic cavernous sinus thrombosis as a complication of sphenoid sinusitis, Ci Ji Yi Xue Za Zhi 31 (1) (2019) 63–65, https://doi.org/10.4103/tcmj.tcmj_1_18.
[6] S. Kasha, G. Bandari, Bilateral posterior fracture-dislocation of shoulder following seizures secondary to cavernous sinus venous thrombosis - a rare association, J. Orthop. Case Rep. 8 (4) (2018) 49–52, https://doi.org/10.13107/jocr.2250-0685.1156.
[7] J. Berge, C. Louail, J.M. Caille, Cavernous sinus thrombosis diagnostic approach, J. Neuroradiol. 21 (2) (1994) 101–117.
[8] B. Schuknecht, D. Simmen, C. Yuksel, A. Valavanis, Tributary venosinus occlusion and septic cavernous sinus thrombosis: CT and MRI findings, AJNR Am. J. Neuroradiol. 19 (4) (1998) 617–626.
[9] R. Ben-Uri, L. Palma, Z. Kaveh, Case report: septic thrombosis of the cavernous sinus: diagnosis with the aid of computed tomography, Clin. Radiol. 40 (5) (1989) 520–522, https://doi.org/10.1016/s0009-9260(89)80272-7.
[10] J. Ahmadi, J.R. Keane, H.D. Segall, C.S. Zee, CT observations pertinent to septic cavernous sinus thrombosis, AJNR Am. J. Neuroradiol. 6 (5) (1985) 755–758.
[11] S.S. Deliran, L. Sondag, Q.H. Leijten, A.M. Tuladhar, F.J.A. Meijer, Headache: consider cavernous sinus thrombophlebitis, Ned. Tijdschr. 16 (2018) 162.
[12] T. Fujikawa, Y. Sogabe, Septic cavernous sinus thrombosis: potentially fatal

conjunctival hyperemia, Intensive Care Med. (2018) 30, https://doi.org/10.1007/s00134-018-5322-6.
[13] N.A. Van der Poel, K.D. de Witt, R. van den Berg, M.M. de Win, M.P. Mourits, Impact of superior ophthalmic vein thrombosis: a case series and literature review, Orbit 38 (3) (2018) 226–232, https://doi.org/10.1080/01676830.2018.1497068.
[14] Y.H. Wang, P.Y. Chen, P.J. Ting, F.L. Huang, A review of eight cases of cavernous sinus thrombosis secondary to sphenoid sinusitis, including a12-year-old girl at the present department, Infect. Dis. (Lond) 49 (9) (2017) 641–646, https://doi.org/10.1080/23744235.2017.1331465.
[15] G.S. Frank, J.M. Smith, B.W. Davies, D.M. Mirsky, E.M. Hink, V.D. Durairaj, Ophthalmic manifestations and outcomes after cavernous sinus thrombosis in children, J. AAPOS 19 (4) (2015) 358–362, https://doi.org/10.1016/j.jaapos.2015.06.001.
[16] J.L. Leach, R.B. Fortuna, B.V. Jones, M.F. Gaskill-Shipley, Imaging of cerebral venous thrombosis: current techniques, spectrum of findings, and diagnostic pitfalls, Radiographics 26 (Suppl 1) (2006) S19–41, https://doi.org/10.1148/rg.26si055174.
[17] K.K. Sabharwal, A.L. Chouhan, S. Jain, CT evaluation of proptosis, Ind. J. Radiol. Imag. 16 (4) (2006) 683–688, https://doi.org/10.4103/0971-3026.32299.
[18] J. Hwang, H.S. Hong, J. Park, A. Lee, E.J. Choo, K.H. Chang, Fulminant superior ophthalmic vein thrombosis and cavernous sinus thrombophlebitis with intracranial extensions: case reports, J. Korean Soc. Ther. Radiol. Oncol. 72 (6) (2015) 418–422, https://doi.org/10.3348/jksr.2015.72.6.418.
[19] A. Abdel Razek, E. Saad, N. Soliman, H. Abou Elatta, Assessment of vascular disorders of the upper extremity with contrast-enhanced MR angiography: pictorial review, J. Radiol. 28 (2) (2010) 87–94, https://doi.org/10.1007/s11604-009-0394-4.
[20] M.Y. Cho, S.H. Park, S.H. Yoon, J.D. Kim, CT and MR findings of cavernous sinus lesions, J. Korean Soc. Radiol. 30 (1) (1994) 19–26.
[21] G. Scotti, C.Y. Yu, W.P. Dillon, et al., MR imaging of cavernous sinus involvement by pituitary adenomas, AJR Am. J. Roentgenol. 151 (4) (1988) 799–806, https://doi.org/10.2214/ajr.151.4.799.
[22] J.R. Ebright, M.T. Pace, A.F. Niazi, Septic thrombosis of the cavernous sinuses, Arch. Intern. Med. 161 (22) (2001) 2671–2676, https://doi.org/10.1001/archinte.161.22.2671.
[23] A.T. Rai, J.P. Hogg, B. Cline, G. Hobbs, Cerebrovascular geometry in the anterior circulation: an analysis of diameter, length and the vessel taper, J. Neurointerv. Surg. (2013), https://doi.org/10.1136/neurintsurg-2012-010314.
[24] Rao v Chaudhary. Dilated superior ophthalmic vein commonly caused by cerebral vascular malformation. American Academy of Ophthalmology.
[25] R. Wei, J. Cai, X. Ma, H. Zhu, Y. Li, Imaging diagnosis of enlarged superior ophthalmic vein, Zhonghua Yan Ke Za Zhi 38 (7) (2002) 402–404.